Fluid Phase Equilibria 500 (2019) 112249

Contents lists available at ScienceDirect

Fluid Phase Equilibria

journal homepage: www.elsevier.com/locate/fluid

Thermodynamic characterization of deep eutectic solvents at high pressures

Emanuel A. Crespo [a], João M.L. Costa [a], André M. Palma [a], Belinda Soares [a], M. Carmen Martín [b], José J. Segovia [b], Pedro J. Carvalho [a], João A.P. Coutinho [a, *]

[a] CICECO, Aveiro Institute of Materials, Department of Chemistry, University of Aveiro, 3810-193, Aveiro, Portugal
[b] BioEcoUVa, Research Institute on Bioeconomy, TERMOCAL Research Group, University of Valladolid, Escuela de Ingenierías Industriales, Paseo del Cauce 59, 47011, Valladolid, Spain

ARTICLE INFO

Article history:
Received 19 May 2019
Received in revised form
5 July 2019
Accepted 19 July 2019
Available online 20 July 2019

Keywords:
Deep eutectic solvents
SAFT
Cholinium chloride
Density
Viscosity

ABSTRACT

Despite the large spectrum of applications being reported for DESs over the last decade, their thermodynamic characterization is often neglected, hindering a better understanding of their nature, and the development of accurate and robust thermodynamic models to describe them, essential for the conceptual and design stages of new industrial processes.

This work aims at decreasing such a gap in literature by reporting new experimental density and viscosity data in wide temperature and pressure ranges for the three archetypal DESs of cholinium chloride, as hydrogen bond acceptor, combined with either ethylene glycol, glycerol, or urea, as hydrogen bond donor. The experimental data measured in this work were then correlated using the Perturbed Chain - Statistical Associating Fluid Theory equation of state coupled with the Free Volume Theory to assess the performance of existing coarse-grained models when applied to the description of DESs. The modelling results obtained highlight the limitation of the existing models, since a correct prediction of DES density could not be achieved, reinforcing the need for viable alternative approaches for the development of coarse-grained models that are appropriate for the thermodynamic modelling of DESs.

1. Introduction

Most industrial processes rely on the use of conventional organic solvents that represent a large share of the total volume of chemicals used. Moreover, these solvents pose environmental, health, and safety challenges, including human and eco-toxicity concerns, process safety hazards, and waste management issues. Hence, with the upsurge of green chemistry, chemists and chemical engineers are expected to explore the full potential and applicability of alternative solvents in an effort towards the development of greener and more sustainable processes.

In the last decade, deep eutectic solvents (DES) have emerged as a new type of green solvents. Firstly proposed by Abbott et al., in 2003 [1], DES are eutectic solvents formed by mixtures of two or more compounds that exhibit a large freezing temperature depression allowing the formation of stable liquids at relatively low temperatures. Although there is still a debate about the meaning of the "deep" qualificative, the advantages of these solvents on different fields are undeniable [2].

DESs are known for their tunable character as the solvent properties can easily be tuned by a proper selection of the DES precursors and their molar ratio. The DESs simple preparation without complex purification steps, liquidus temperatures allowing operation under mild conditions, and biocompatibility granted them the interest from both industry and academia with several applications for DESs being reported in the literature [3,4]. Such applications include, but are not limited to, organic synthesis [5–7], biocatalysis [8,9], electrochemistry [10,11], separation of gases [12,13], conversion of lignocellulosic biomass [14], extraction of glycerol from biodiesel [15], extraction media for azeotropic mixtures [16], fuel purification [17], drug vehicles [18], and preparation of nanomaterials [19].

Moreover, the low cost and availability of the most common constituents of DESs is another great advantage of these solvents. A wide range of possible hydrogen bond donor (HBD) and hydrogen bond acceptor (HBA) precursors have been proposed and extensive lists of DES can be found in the literature [3,12,20–22]. As HBDs, a

* Corresponding author.
E-mail address: jcoutinho@ua.pt (J.A.P. Coutinho).

https://doi.org/10.1016/j.fluid.2019.112249
0378-3812/

wide variety of amines [23], amides [24], carboxylic acids [25–29], alcohols or polyols [30,31], amino acids [32,33], urea and its derivatives [1,18] or sugars [34,35] can be used, with natural products representing a plentiful and ideal source of DESs precursors due to their enormous chemical diversity, biodegradability, sustainability, and toxicity profile. The HBAs are normally organic salts, typically quaternary ammonium salts, with cholinium chloride ([Ch]Cl) being the most common due to its biocompatibility and low cost.

With the widening of applications for DESs, a reliable knowledge of their thermophysical properties (e.g. density and viscosity) is required for an accurate design, simulation and optimization of any new industrial process. However, the large literature body on DES applications has not been followed by a similar effort in providing an extensive thermodynamic characterization of these solvents. Moreover, the lack of such fundamental data, important for a better understanding of the DES nature, has been hindering the development of accurate and robust thermodynamic models needed by process simulation software.

Even for the more common [Ch]Cl-based DESs such as the archetypal mixtures of [Ch]Cl with ethylene glycol (EG), glycerol and urea, such extensive studies are scarce and usually carried in narrow temperature and pressure ranges. Although a few authors reported density data at atmospheric pressure for the mixture with EG Refs. [36–43], glycerol [37,38,40,42,44,45], and urea [36,46,47], in the (283.15–373.15) K temperature range, only Leron and coworkers [48–50] reported density values at higher pressures (up to 50 MPa) but in a narrower temperature range, namely (298.15–323.15) K. Regarding viscosity, several authors reported values at atmospheric pressure for the mixture with EG Refs. [36,42,43,51], glycerol [42,44,45,52], and urea [36,46,47,51] in the (293.15–363.15) K temperature range but, to the best of our knowledge, no measurements were previously reported at higher pressures.

Likewise, the thermodynamic modelling of DESs is a poorly explored research subject due to the complex hydrogen bonding interactions governing these systems that represent a challenge for most current models, but also because of the limited reliable experimental data. Molecular-based equations of state (EoSs) derived from the Statistical Associating Fluid Theory (SAFT) [53,54] able to explicitly account for specific molecular effects such as hydrogen-bonding and polar interactions have been suggested by different authors as the most appropriate tool for the modelling of DESs.

Verevkin et al. [55] used the PC-SAFT EoS to model the infinite dilution activity coefficients of different solutes in [Ch]Cl + glycerol DES while Zubeir et al. [56] applied the same model to describe the solubility of CO_2 in DESs composed of tetraalkylammonium chlorides ([TXA][Cl]) and lactic acid (LA). Both a pseudo-pure component approach and an individual-component approach were applied in this work and good correlations of the experimental data were obtained. However, the molecular parameters for the DES and the binary interaction parameters applied using the pseudo-pure-component approach were necessarily dependent on the HBD/HBA ratio requiring an individual fitting to each composition. Despite this disadvantage, the same approach was later used to predict the CO_2 solubilities in hydrophobic DESs composed of quaternary ammonium salts and decanoic acid [57], and to investigate the selective removal of thiophene from oil using DESs [58]. The same approach was used by Haghbakhsh et al. [59] who applied the CPA EoS to study the solubility of CO_2 in fifteen different DES.

Another major drawback of using a pseudo-pure component approach to describe DESs is its inability to describe the solid-liquid equilibrium (SLE) of the eutectic mixture, which is of utmost importance for a better understanding of DESs nature. Hence, Crespo et al. [28,29,60] applied the PC-SAFT EoS, following an individual-component approach, to satisfactorily correlate the SLE of several DESs composed of different quaternary ammonium chloride salts as HBA and carboxylic acids or alcohols as HBD. This more realistic approach was also applied by Ojeda and Llovell [61] that used the soft-SAFT EoS to correlate the solubilities of CO_2 and SO_2 in DESs.

A clear advantage of SAFT-type EoSs is that they can be easily coupled with different theories for the calculation of properties other than phase equilibria, such as transport or interfacial properties. Both the Free Volume Theory (FVT) [62,63] and the friction theory [64,65] have recently been coupled with either PC-SAFT, soft-SAFT, or CPA for the description of DESs viscosities [66–68]. However, results were only reported under a pseudo-pure component approach.

Therefore, the aim of this work is two-fold: Firstly, the densities and viscosities of the three archetypal DESs: [Ch]Cl with either EG, glycerol or urea are measured in extensive temperature and pressure ranges to decrease the gap on the existent literature body and to investigate the effect of both temperature and pressure upon these fundamental properties. Then, the PC-SAFT EoS coupled with the FVT is applied under an individual component approach, using coarse-grained models available in literature, to describe the experimental data, assessing the capability of existing models to capture the DESs thermophysical properties.

2. Experimental section

2.1. Materials

High-pressure densities and viscosities were measured for eutectic mixtures of [Ch]Cl and EG, glycerol or urea. [Ch]Cl was acquired from Acros Organics with a mass fraction purity higher than 98% and further dried under vacuum (0.1 Pa) and moderate temperature (298.15 K) for a period never smaller than 72 h. Ethylene glycol, glycerol, and urea were acquired from Fluka, Acros Organics and Sigma Aldrich, respectively, with mass fraction purity higher than 99%. To remove traces of water, individual samples of each compound were dried, and their water content, determined with a Metrohm 831 Karl Fischer coulometer (using the Hydranal-Coulomat AG from Riedel-de Haens as analyte), are reported in Table 1. The purity of each compound was checked by ^{1}H and ^{13}C NMR. The full name, chemical structure, CAS number, molecular weight, average water content, mass purity, and supplier of each compound are reported in Table 1.

2.2. Eutectic mixtures preparation

The eutectic mixtures, reported in Table 2, were prepared, analytically, inside a dry-argon glove-box, by weighting the desired amount of each pure compound using an analytical balance model ALS 220-4N from Kern with a reproducibility of 0.0002 g. The vials were closed using a Teflon stopper and the mixtures heated until melting and complete dissolution, under stirring, to assure complete homogenization.

The water content of the eutectic mixtures was measured prior to the density and viscosity measurements using the Metrohm 831 Karl Fischer coulometer and are also reported in Table 2.

2.3. Density measurements

Densities were measured in the (283–363) K temperature and (0.1–95) MPa pressure ranges using a DMA-HPM, coupled with a mPDS 5 unit, high-pressure densimeter from Anton Paar. The standard uncertainty on the density was found to be $5 \cdot 10^{-4}$ g cm^{-3}

Table 1
Chemical structure, CAS number, molecular weight, supplier and purity of the compounds studied in this work.

Compound	Chemical structure
Ethylene glycol (EG) (CAS: 107-21-1; Mw = 62.07 g mol-1; wt% = 99.5%; w_{H2O} < 30 ppm) acquired from Fluka	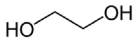
Glycerol (CAS:56-81-5; Mw = 92.09 g mol-1; wt% = 99%; w_{H2O} < 30 ppm) acquired from Acros Organics	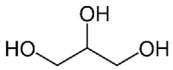
Urea (CAS:57-13-6; Mw = 60.06 g mol-1; wt% = 99.5%; w_{H2O} < 100 ppm) acquired from Sigma Aldrich	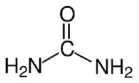
Cholinium chloride ([Ch]Cl) (CAS:67-48-1; Mw = 139.62 g mol-1; wt% = 98%; w_{H2O} < 639 ppm) acquired from Acros Organics	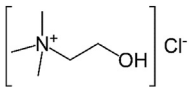

Table 2
Eutectic solvents prepared in this work.

Eutectic Mixture (1:2): [Ch]Cl (1) +	
density measurements	viscosity measurements
EG (w_1 = 0.529; x_1 = 0.333; w_{H2O} < 240 ppm)	**EG** (w_1 = 0.537; x_1 = 0.340; w_{H2O} < 240 ppm)
Glycerol (w_1 = 0.431; x_1 = 0.333; w_{H2O} < 290 ppm)	**Glycerol** (w_1 = 0.431; x_1 = 0.333; w_{H2O} < 290 ppm)
Urea (w_1 = 0.535; x_1 = 0.331; w_{H2O} < 200 ppm)	**Urea** (w_1 = 0.529; x_1 = 0.326; w_{H2O} < 200 ppm)

[69]. The measuring cell was thermostatized by circulating a heat-carrier fluid thermo-regulated, using a thermostat bath circulator (Julabo MC) with a temperature stability of 0.01 K and uncertainty of 0.1 K. Pressure was monitored using a piezoresistive silicon pressure transducer (Kulite HEM 375) with an accuracy better than 0.2% and fixed directly in a stainless-steel line, in order to reduce dead volumes, and placed between the DMA-HPM cell and a movable piston.

A detailed description of the apparatus, methodology and calibration procedure can be found elsewhere [69].

2.4. Viscosity measurements

Two approaches were used to determine the mixtures' density. One, using a SVM3000 rotational Stabinger viscometer-densimeter, from Anton Paar, and other using a falling body viscometer. Using the automated SVM3000 Anton Paar rotational Stabinger viscometer-densimeter, dynamic viscosity (η) was determined in the temperature range from (293.15−373.15) K and at atmospheric pressure (0.1 ± 0.01 MPa) within a standard uncertainty on the dynamic viscosity of 2% and 0.02 K on the temperature. Further details regarding the equipment and adopted methodology can be found elsewhere [70].

The viscosity measurements as function of pressure were obtained using a falling body viscometer developed and implemented in TERMOCAL laboratory and shown to be able to adequately describe a large set of compounds' families [71,72]. This equipment operation is based on the falling body measurement through a vertical tube containing the fluid whose viscosity is sought and is able to measure viscosity in wide (0.1−140) MPa and (253.15−523.15) K pressure and temperature ranges, respectively. Viscometer calibration was performed at p = (0.1−100) MPa and T = (293.15−393.15) K with water and n-dodecane. The relative expanded uncertainty was found to vary from 2.5% to ±3.5% for the highest and lowest viscosity limits, respectively [71−73].

3. Thermodynamic modelling

3.1. PC-SAFT EoS

PC-SAFT, proposed by Gross and Sadowski in 2001 [74], is one of the most used variants of the Statistical Associating Fluid Theory EoS, developed by Chapman et al. [53,54,75,76] based on Wertheim's first-order thermodynamic perturbation theory (TPT1) [77−80]. SAFT-type EoSs are based on statistical mechanics concepts and are able to explicitly account for the effect of different structural and energetic effects (e.g. anisotropic associative interactions, electrostatics …) on the thermodynamic behavior of a fluid.

SAFT represents molecules as a number of equally-sized spherical segments, or monomers, covalently bonded to each other forming chains that may or may not associate at specific short-range bonding sites. The model is then written as a sum of different terms to the residual Helmholtz energy of the system, A^{res}, with each of these terms describing a specific contribution. Such additivity is illustrated in eq. (1), where A^{seg} represents a contribution due to the monomer-monomer interactions (repulsive and attractive), A^{chain}, represents a contribution due to the formation of chains from the spherical monomers, and A^{assoc} a contribution due to the short-range and highly directional associating forces such as hydrogen bonding. Given the additivity characterizing SAFT models, additional terms can be included depending on the systems nature, to better capture their physical features. An example is the frequent addition of a polar term, A^{polar}, to explicitly account for polar and multipolar interactions.

$$\frac{A^{res}}{Nk_BT} = \frac{A^{seg}}{Nk_BT} + \frac{A^{chain}}{Nk_BT} + \frac{A^{assoc}}{Nk_BT} + \frac{A^{polar}}{Nk_BT} + \ldots \quad (1)$$

PC-SAFT, contrarily to the original SAFT model, uses a hard-chain reference fluid instead of hard spheres. This reference fluid

consists on a number of m_i^{seg} freely jointed monomers exhibiting no attractive interactions, and accounts for the shape and length of molecules, and the repulsive interactions between monomers. Therefore, eq. (1) is slightly modified into eq. (2), where A^{hc} represents the contribution due to the hard-chain reference fluid, and A^{disp} accounts for the dispersive interactions between the monomeric segments. As polar gases and aromatics will not be studied in this work, the polar term is neglected throughout this work.

$$\frac{A^{res}}{NkT} = \frac{A^{hc}}{NkT} + \frac{A^{disp}}{NkT} + \frac{A^{assoc}}{NkT} \tag{2}$$

The term A^{disp} is derived from the perturbation theory of Barker and Hendersen [81,82], and introduces two additional parameters; the diameter of the monomeric segments, σ_{ii}, and the dispersive energy characterizing the monomer-monomer interactions, u_{ii}/k_B. Therefore, three pure-component parameters are necessary to model a non-associating component in PC-SAFT. The extension to mixtures is carried using the van der Waals one fluid theory employing the Lorentz-Berthelot mixing rules:

$$\sigma_{ij} = \frac{\sigma_{ii} + \sigma_{jj}}{2} \tag{3}$$

$$u_{ij} = (1 - k_{ij})\sqrt{u_{ii}u_{jj}} \tag{4}$$

A binary interaction parameter, k_{ij}, correcting deviations from eq. (4), may be introduced when required to achieve quantitative agreement with the experimental data.

The association term is particularly important in the modelling of DES given the important role of hydrogen bonding in these systems. Its evaluation requires two additional parameters; the association energy, ε_{ii}^{HB}, and volume, κ_{ii}^{HB} of the square-well bonding sites. The extension of the association term to mixtures requires the value of the cross-association parameters, which are obtained from the self-associating parameters using appropriate combining rules such as those proposed by Wolbach and Sandler [83].

$$\varepsilon^{A_iB_j} = \frac{\varepsilon_{ii}^{HB} + \varepsilon_{jj}^{HB}}{2} \tag{5}$$

$$\kappa^{A_iB_j} = \sqrt{\kappa_{ii}^{HB}\kappa_{jj}^{HB}}\left(\frac{\sqrt{\sigma_{ii}\sigma_{jj}}}{1/2(\sigma_{ii} + \sigma_{jj})}\right)^3 \tag{6}$$

For further details on the PC-SAFT EoS and the different terms of eq. (2), the reader is directed to the original paper by Gross and Sadowski [74]. All the PC-SAFT calculations carried in this work were performed using the software Multiflash 7.0 by KBC-Infochem, using coarse-grained models and parameters previously reported in literature and discussed in the next section.

3.2. PC-SAFT coarse-grained models

The robustness and accuracy of SAFT-type EoSs like PC-SAFT rely on the careful development of the coarse-grained models representing each compound present in the system. These coarse-grained models should be able to capture most of the compounds' physical features and include both a proper fitting of the pure-component parameters but also the definition of the association scheme. The association scheme defines the number and type of association sites present in the molecule and the interactions allowed in the system, for which the association energy and volumes have to be defined pairwise.

All four components studied in this work were previously modelled using PC-SAFT. Zubeir et al. [56] proposed a coarse-grained model for [Ch]Cl using the 2B association scheme (one positive and one negative association sites) to describe the CO_2 solubilities in DES while Held and co-workers [84,85] presented a model for glycerol and urea also using the 2B scheme. For ethylene glycol, several sets of molecular parameters are available in the literature such as those reported by Atilhan and Aparicio [86], Reschke et al. [87], and Liang et al. [88] As density is one of the properties to be described in this work, these three CG models for EG were evaluated through the prediction of the $p\rho T$ data reported by Crespo et al. [69] The results of those calculations for three different isotherms are illustrated in Fig. 1, while the results for the remaining isotherms reported by Crespo et al. [69] can be found in Fig. S1, in Supporting Information. As can be observed in Fig. 1, only the PC-SAFT parameters proposed by Atilhan and Aparicio [86] are able to correctly describe the effect of both temperature and pressure on the densities of EG. On the contrary, the other two sets of parameters yield inaccurate results even at atmospheric pressure. The percentage average absolute deviations (%AARD) of the PC-SAFT predictions were calculated through eq. (7) and equal to 0.1898%, 1.301%, and 2.628%, when using the parameters reported by Atilhan and Aparicio [86], Reschke et al. [87], and Liang et al. [88], respectively. Hence, the model and parameters proposed by Atilhan and Aparicio [86] were adopted in this work. These parameters and those considered for the remaining components are summarized in Table 3.

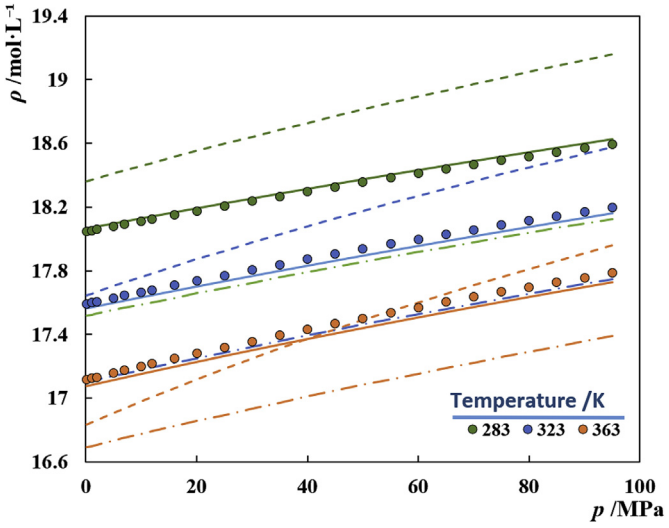

Fig. 1. High-pressure liquid densities of pure EG. Symbols represent experimental data [69] while the solid, dashed and long-dash-dotted lines represent the PC-SAFT predictions using the parameters proposed by Atilhan and Aparício [86], Reschke et al., [87] and Liang et al. [88].

$$\%AARD(\rho) = 100\frac{\left|\rho^{\exp} - \rho^{calc}\right|}{\rho^{\exp}} \tag{7}$$

Table 3
PC-SAFT pure-component parameters considered in this work. N_{sites} represent the number of donor/acceptor associating sites.

Component	M_w/g·mol^{-1}	N_{sites}	m_i^{seg}	σ_i/Å	u_i /K	ε^{AiBi} /K	κ^{AiBi}
[Ch]Cl [56]	139.62	1/1	13.02	2.368	228.07	8000	0.200
EG [86]	62.07	1/1	2.4366	3.2328	344.06	2702.6	0.02216
Glycerol [85]	92.09	1/1	2.007	3.815	430.82	4633.5	0.0019
Urea [84]	60.06	1/1	4.244	2.446	368.23	3068.3	0.0010

3.3. Free volume theory (FVT)

One of the most popular approaches to model the viscosity of dense fluids is the free volume theory (FVT) proposed by Allal et al. [62,63] based in earlier concepts of free volume and diffusion. According to this theory, viscosity is given as a sum of two terms (eq. (8)): the diluted gas term, η_0, and the dense-state correction term, $\Delta\eta$, in an approach similar to that proposed by Quiñones-Cisneros et al. [64] for the friction theory, to isolate the purely kinematic physics of the diluted gas limit from the dense-state physics.

$$\eta = \eta_0 + \Delta\eta \tag{8}$$

The first term, describes the viscosity of a fluid with a very low density using a modified version of the original Chapman-Enskog theory proposed by Chung et al. [89] in the following expression:

$$\eta_0 = 40.785 \times 10^{-4} \frac{\sqrt{M_w T}}{v_c^{2/3} \times \Omega^*(T^*)} F_c \tag{9}$$

where η_0 is the viscosity of the diluted gas in cP, T is the temperature in K, M_w the molecular weight in g/mol and v_c the critical volume in cm^3/mol, Ω^* is the reduced collision integral that is evaluated at a dimensionless temperature $T^* = 1.2593T/T_c$ (T_c is the critical temperature in K), from the expression proposed by Neufeld et al. [90], F_c is a correction factor to include the effects of chain bonding, hydrogen bonding and polarity that was introduced by Chung et al. [89] as a function of the acentric factor, ω, a dimensionless dipole moment of the molecule, μ_r, and a parameter κ that accounts for hydrogen bonding:

$$F_c = 1 - 0.2756\omega - 0.059035\mu_r^4 - \kappa \tag{10}$$

In the case of mixtures, the contribution of each component to the diluted-gas term is first calculated independently and then a general equation for multicomponent systems proposed by Wilke [91] is used to sum the different contributions:

$$\eta_0^{mix} = \sum_{i=1}^{NC} \frac{\eta_0^i}{1 + \frac{1}{x_i} \sum\limits_{\substack{j=1 \\ j \neq i}}^{NC} x_j \phi_{ij}} \tag{11}$$

where NC is the number of components, x_i the molar fraction of component i, and ϕ_{ij} is given by the following expression:

$$\phi_{ij} = \frac{\left[1 + \left(\eta_0^i / \eta_0^j\right)^{1/2} \left(M_w^i / M_w^j\right)^{1/4}\right]^2}{\left(4/\sqrt{2}\right)\left[1 + \left(M_w^i / M_w^j\right)\right]^{1/2}} \tag{12}$$

In this work the diluted-gas term is neglected as the necessary critical properties are not available for [Ch]Cl. Moreover, the contribution of this term for the calculation of liquid viscosities is typically small, and may be neglected [92].

The dense-state term is believed to be connected to the molecular structure of the fluid and exponentially dependent on the empty space (free volume) between molecules. The final expression is given in eq. (13):

$$\Delta\eta = L_v\left(0.1p + 10^{-4}\alpha\rho^2 M_W\right)\sqrt{\frac{10^{-3}M_w}{3RT}}\exp\left[B\left(\frac{10^3 p + \alpha\rho^2 M_W}{\rho RT}\right)^{3/2}\right] \tag{13}$$

where $\Delta\eta$ is the dense-term contribution to viscosity in cP, p is the pressure in MPa, ρ is the density in mol/L and R is the ideal gas constant in $J\cdot K^{-1}\cdot mol^{-1}$. Eq. (13) includes three adjustable parameters: L_v which is a length parameter related to the molecule's structure and relaxation time, B the free-volume overlap, and α that is related to the energy barrier. These parameters must be fitted to the available experimental viscosity data and, whenever possible, related to the molecular weight if the compounds belong to the same chemical family.

The extension to mixtures requires the evaluation of the three parameters for the mixture through appropriate mixing rules. Given that there is still disagreement about the best mixing rule to be used with the FVT [93–99], in this work we employ the simplest one where the different parameters depend linearly on the mixture composition without using any binary parameters in the viscosity treatment.

$$\alpha^{mix} = \sum_{i=1}^{NC} \alpha_i x_i \tag{14}$$

$$B^{mix} = \sum_{i=1}^{NC} B_i x_i \tag{15}$$

$$L_v^{mix} = \sum_{i=1}^{NC} L_{v,i} x_i \tag{16}$$

The calculation of viscosity requires the previous calculation of some thermodynamic properties, namely the density and pressure/temperature of the system through an appropriate EoS. Therefore, the accuracy of the calculated viscosities is greatly influenced by the accurate calculation of those properties by the chosen EoS.

4. Results

The density of the three archetypal [Ch]Cl-based DES ([Ch]Cl combined with either EG, glycerol, or urea at a stoichiometric ratio of 1:2) were measured in this work at temperatures ranging from (283–363) K and pressures from (0.10–95) MPa.

For the mixture with EG, several authors reported density data at atmospheric pressure in the (293–363) K temperature range [36–43] while for the system with glycerol, data was reported in the (283–363) K temperature range [37,38,40,42,44,45]. Despite [Ch]Cl + urea (1:2) being the first DES reported and one of the most used [1], density data is much scarcer [36,46,47].

As shown in Fig. 2, a good agreement between the atmospheric pressure data reported in this work and those reported in literature for the three mixtures is found with percentage average relative deviations (%ARD – eq. (17)) mostly in the range of ±0.3%, resulting in density differences lower than 0.005 g cm^{-3}. Overall, small and nonsystematic deviations were found between the different references except for the density data reported by Popescu et al. [39] and Mjalli et al. [42] for the mixture with EG.

The former reports density values significantly lower than those reported in this work, a possible explanation being a higher water content of the samples with the authors reporting a maximum of

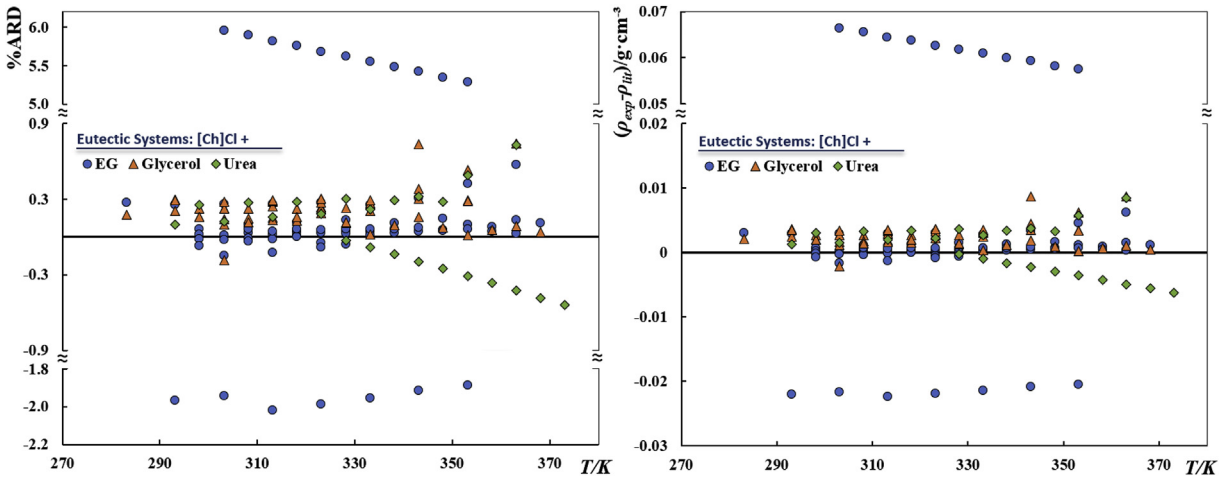

Fig. 2. Percentage average relative deviations (%ARD) (left) and density differences (right) between density data at atmospheric pressure measured in this work and those reported in literature [36–47]

5% in weight which is significantly higher than those reported in this work. Unfortunately, important details concerning sample preparation (e.g. drying of [Ch]Cl, use of a glove box to prepare the mixtures, …) were not provided by the authors. On the other hand, the data of Mjalli et al. [42] shows density values considerably higher than those reported in this work and the other literature references, including those reported by the same author a few years earlier [40]. However, no discussion about such differences was provided by the authors in their last work.

$$\%ARD(\rho) = 100\frac{\rho^{\exp} - \rho^{lit}}{\rho^{\exp}} \quad (17)$$

While density data for these mixtures at atmospheric pressure is widely available in literature, $p\rho T$ data is much scarcer. To the best of our knowledge, only Leron and co-workers [48–50] reported density data for these three mixtures at higher pressures (up to 50 MPa) but, unfortunately, in a narrower temperature range, namely (298–323) K. As shown in Fig. 3 a good agreement between the experimental data measured in this work and that reported by Leron and co-workers [48–50] was found with %ARD lower than 0.25% and density differences below 0.003 g cm^{-3}. Most of our data shows density values higher than those reported in literature with the deviations increasing with the HBD in the order EG < urea < glycerol.

For the mixture with glycerol where the deviations are the highest, the literature values seem to be shifted +5 K (i.e., the densities reported at 318 K are overlapped with those measured in this work at 323 K). This is shown in Fig. S2 of Supporting Information.

Overall, the small density differences observed can be related to the water content of the DES and small differences on the weighted masses of both components, i.e. the final HBD/HBA ratio of the studied DES.

The density values measured in this work are depicted in Fig. 4 along with the PC-SAFT modelling results and reported in tabular form in Tables S1–S3 of Supporting Information.

Urea is the only HBD studied in this work which remains solid at temperatures higher than room temperature, so pure fluid liquid densities are not available. However, the density of urea near its melting point is available in the DIPPR database [100] having the value of 1.23 g cm^{-3} at 405.85 K. According to the same source, the density of pure ethylene glycol and glycerol at that same temperature is 1.028 and 1.185 g cm^{-3}, respectively. Accordingly, densities

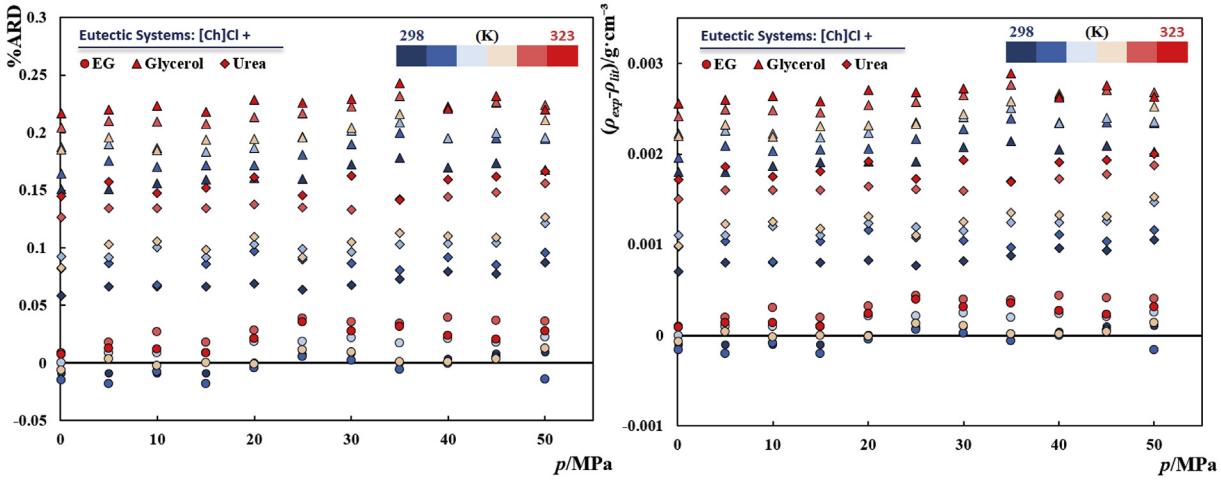

Fig. 3. Percentage average relative deviations (%ARD) (left) and density differences (right) between density data at pressures up to 50 MPa measured in this work and those reported in literature [48–50].

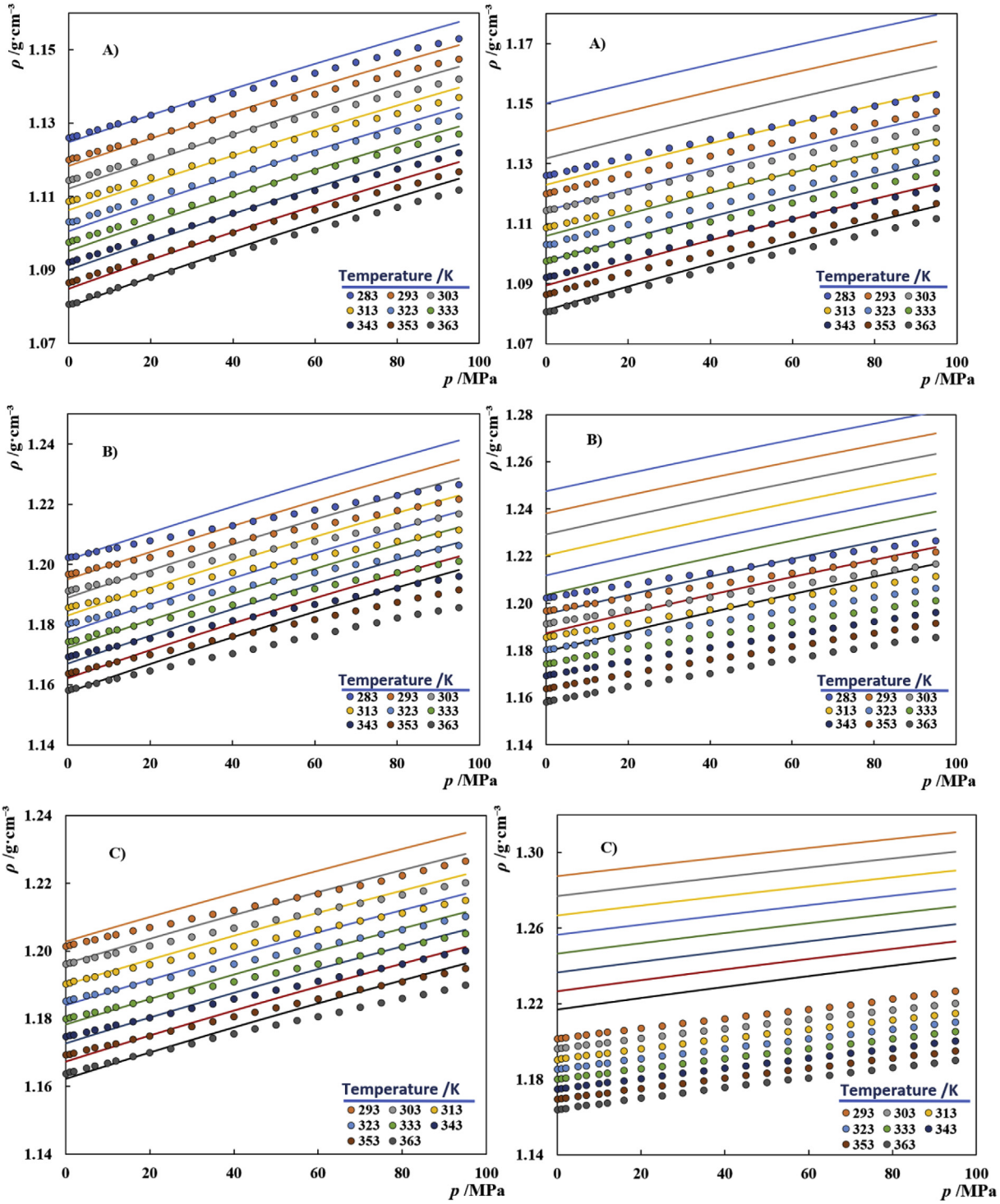

Fig. 4. High-pressure densities of [Ch]Cl-based DES with A) ethylene glycol B) glycerol C) urea as hydrogen bond donor. Symbols represent the experimental data measured in this work while the solid lines depict the PC-SAFT correlation of the data using a temperature-dependent binary interaction parameter (left) or the PC-SAFT predictions ($k_{ij} = 0$) of the data (right).

measured in this work were found to increase with the HBD in the same order as the pure compounds: EG < glycerol < urea. This was expected considering that the molar volume is usually an additive property and that the HBA is [Ch]Cl in all cases, which, at the same temperature, has a density of 1.0454 g cm^{-3}, if extrapolated from the densities of aqueous solutions reported by Francisco et al. [101].

Furthermore, extrapolating the data measured in this work to 405.85 K, taking advantage of the property linear dependency with temperature, the excess molar volumes of the three eutectic solvents were estimated in 3.77, −9.11, and −1.16 cm^3/mol for the mixtures with EG, glycerol, and urea, respectively. Even though the excess molar volumes and excess Gibbs energy of the system can exhibit opposite behaviors, the negligible excess molar volume of the mixture with urea is in a good agreement with the quasi-ideal

behavior observed for [Ch]Cl in urea, previously reported [2,102]. Moreover, the excess molar volumes obtained suggest the existence of stronger favorable interactions for the glycerol mixture and, surprisingly, less favorable interactions for the mixture with EG. The existence of this enthalpic effect in the eutectic solvent containing glycerol is corroborated by the significative negative deviations from the ideal behavior observed by Abbott et al. [103] when measuring the solid-liquid equilibrium for this system.

Based on the additive character of density, when excess volumes are small, if a thermodynamic model accurately describes the density of all pure components present in a system, which is often the case, as density is normally one of the properties used in the model parameterization, the density of the mixture is at least reasonably well described by the model without any binary interaction parameters. However, from the PC-SAFT coarse-grained models presented in section 3.2, only the model for EG was regressed using pure-component density data.. For the remaining compounds, experimental data from very diluted aqueous solutions (typically at molar fractions of the target compound lower than 0.3) were used in the parameterization procedure.

Considering that the thermodynamic modelling of aqueous systems is a challenging task to any thermodynamic model, and that the interactions present in water are expected to be much different than those observed in other media, the models developed based on diluted aqueous solutions data are unlikely to provide a satisfactory description of the physical features of the target compound, negatively affecting the description of mixtures other than their aqueous solutions. Accordingly, and as observed in Fig. 4 **(right)**, PC-SAFT predictions exhibit considerable deviations from the experimental density data measured in this work, especially for the mixtures with glycerol and urea. These results highlight that alternative approaches are required for a proper modelling of DESs, as coarse-grained models of compounds that are solid at room temperature, developed in the framework of different subjects, are inappropriate to describe even the simplest thermophysical properties of this class of solvents.

To improve the agreement with the experimental data and correct the description of the temperature effect on the density values calculated by PC-SAFT, a linear temperature dependent binary interaction parameter, k_{ij}, correcting the mixture's dispersive energy was used. Although a constant k_{ij}would have been preferred, it was insufficient to describe the temperature effect upon the DES densities. Hence, the final values of the binary parameters applied are summarized in Table 4 while the results of such correlations are depicted in Fig. 4 **(left)**. Using such parameters, a good description of the experimental data was obtained with an overall %AARD of only 0.270%. Again, the best results were obtained for the mixture with EG since the densities of pure EG, including at high pressures, were considered in the parameterization of its model. The highest deviations were observed for the mixture with glycerol since, although both coarse-grained models of glycerol and urea were regressed from diluted aqueous solution data (including densities), higher deviations were reported for the description of the glycerol + water densities than for the aqueous solution of urea [84,85].

Table 4
Binary interaction parameters used in the PC-SAFT correlations of $p\rho T$ data.

	$k_{ij} = a + bT/K$		
	a	*b*	%AARD
[Ch]Cl + EG (1:2)	0.6033	−0.001645	0.131
[Ch]Cl + Glycerol (1:2)	0.6862	−0.001599	0.415
[Ch]Cl + Urea (1:2)	0.9800	−0.002103	0.265
		Mean	0.270

Once the description of the experimental $p\rho T$ data is achieved, the FVT can be coupled with PC-SAFT for the correlation of the DESs viscosities measured in this work. Viscosities of the three [Ch]Cl-based DESs were measured in this work at temperatures ranging from (313−373) K and pressures from (0.10−100) MPa using a falling-body viscometer and are reported in the tabular form in Table S4, in Supporting Information. Viscosities at atmospheric pressure were further compared with viscosities measured using a SVM3000 rotational Stabinger viscometer—densimeter in the (293−373) K temperature range, reported in Table S5. The good agreement between the two sets of experimental data is shown in Fig. 5, validating the data acquired using the falling body viscometer. As observed in Fig. 5, viscosities were found to increase with the HBD in the order EG < glycerol < urea, with the mixtures containing glycerol or urea exhibiting a sharp increase in viscosity as temperature decreases. The higher viscosity of the mixture with urea when compared with the system with glycerol suggests the existence of an important entropic contribution to viscosity as this property shows the opposite behavior to what was expected considering the highly negative excess molar volume of the [Ch]Cl + glycerol DES.

Despite the wide number of applications being reported for these [Ch]Cl-based DES and the importance of an accurate knowledge of their viscosity for several heat and mass transfer purposes, viscosity data is still scarce. Although several authors reported viscosity data at atmospheric pressure for the mixture with EG Refs. [36,42,43,51], glycerol [42,44,45,52], and urea [36,46,47,51], to the best of our knowledge, no data was ever reported at higher pressures.

Data measured in this work at atmospheric pressure is plotted against literature data in Fig. 6.

Overall, a good agreement with the literature data is observed, especially for the mixture with urea. On the contrary, some significant discrepancies are observed in the mixture with glycerol for which the viscosities reported in this work are higher than those observed in literature. Again, the absorption of water by these hydrophilic DESs during manipulation, which is known to occur to a great extent [104], can help to explain such differences. However, most authors do not report water content measurements by Karl-Fischer or other technique prior or after the measurements,

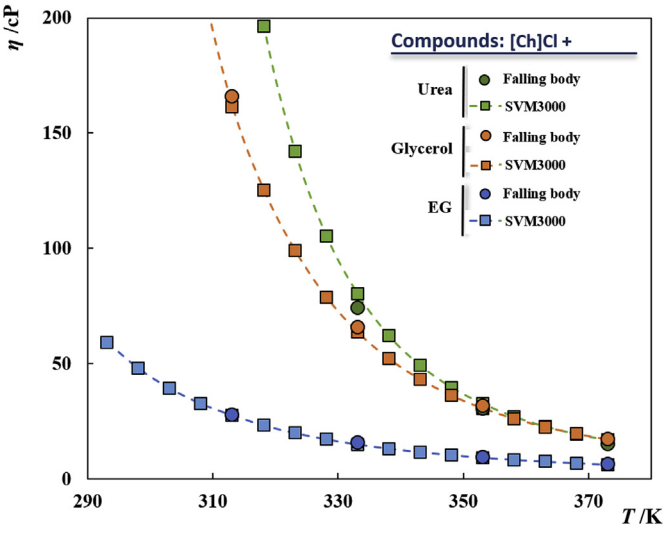

Fig. 5. Viscosities at 0.1 MPa for [Ch]Cl-based DES measured in this work. Circles represent the experimental data measured using the falling body viscometer while the squares with dashed lines represent the data measured using the SVM3000 device.

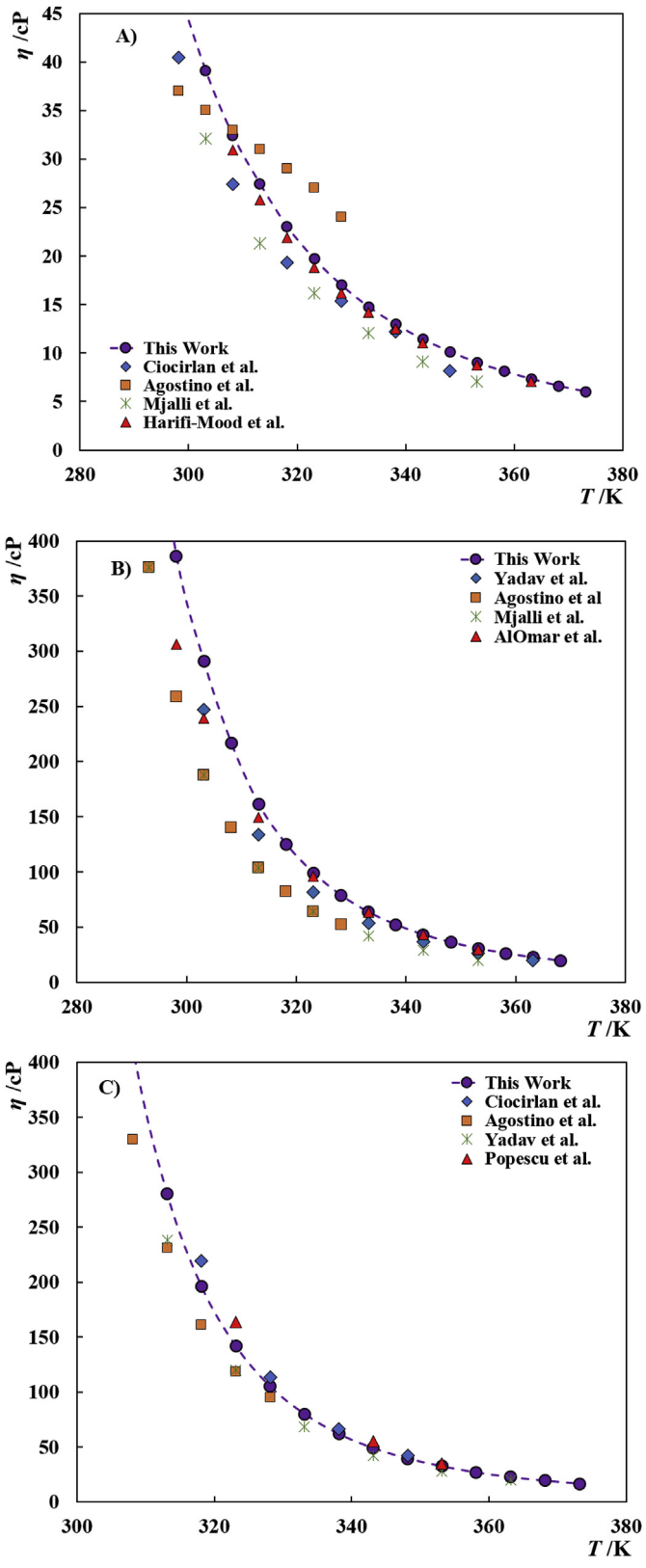

Fig. 6. Viscosities of [Ch]Cl-based DES with different HBDs: A) EG; B) glycerol and C) urea. Symbols represent literature data [36,42–47,51] while the circles with dashed lines depict the data measured in this work.

hindering an adequate discussion on those discrepancies. Nonetheless, a remarkable agreement with the data of AlOmar et al. [45] is observed at higher temperatures. For the mixture with EG, a reasonable agreement with most references is observed except for the data from Agostino et al. [51] which clearly falls off the trend observed in this work and in the other literature sources.

The viscosity data measured in this work at pressures higher than atmospheric, using the falling body viscometer, are plotted in Fig. 7 along with the PC-SAFT + FVT correlations of the data. To correlate the mixture viscosity data, FVT parameters (α, B, and L_v) for each of the pure-components are required, these being typically regressed from pure fluid viscosity data.

Sagdeev et al. [105] measured the viscosities of pure EG in the (0.098–245.2) MPa pressure and (312.5–464.4) K temperature ranges while viscosity data for pure glycerol at atmospheric pressure can be retrieved from the DIPPR database [100]. Both sets of experimental data were used to obtain the FVT parameters for EG and glycerol listed in Table 5 with the results of the fitting being depicted in Figs. S3–S4, showing mean absolute deviations (MAD – eq. (18)) from the experimental data of 0.255 and 1.52 cP, respectively. The higher deviations observed in the system with glycerol, even though only data at atmospheric pressure was considered, demonstrates that although FVT contains three adjustable parameters, a good description of the pure fluid density is still highly relevant to obtain a good correlation of pure fluid viscosity data.

Given the solid nature of [Ch]Cl, viscosity data of the pure component is not available to regress the FVT parameters and thus, viscosity data from [Ch]Cl containing mixtures were used. Hence, and with hindsight of the FVT parameters for EG and glycerol, FVT parameters for [Ch]Cl, listed in Table 5, were regressed from the viscosity data measured in this work using the falling body viscometer for the binary mixtures [Ch]Cl + EG (1:2) and [Ch]Cl + glycerol (1:2) at atmospheric pressure. The results of the fitting are shown in Fig. S5 of Supporting Information and show an excellent agreement with the experimental data with a MAD of only 0.923 and 0.859 cP for the mixtures with EG and glycerol, respectively.

Finally, knowing the FVT parameters for [Ch]Cl, and given the insufficient data measured at atmospheric pressure using the falling body viscometer for the [Ch]Cl + urea (1:2) mixture (i.e. only three experimental points available), the experimental data measured using the SVM3000 was also considered to obtain the FVT parameters for urea reported in Table 5. However, when the whole temperature range of SVM measurements, (293–373) K, was considered, different optimization routines were tested and found to converge to unphysical values of the FVT parameters (e.g. α tending to very low values near zero or L_v exhibiting negative values). Therefore, the optimization was carried considering solely the experimental data in the range of (313–373) K. The results of the optimization procedure are plotted in Fig. S6 and clearly show the difficulties of the model to describe the low temperature viscosities of this mixture. Nonetheless, in the temperature range where the falling body viscometer measurements were carried at higher pressures, i.e. (333–373) K the MAD is only 1.61 cP.

Instead of decreasing the temperature range where the correlation is valid, another alternative would have been the use of a temperature-dependent parameter. Preliminary calculations, not shown here, indicate that using a temperature-dependent B allows to obtain good correlations of the experimental data but, given the increase in the number of adjustable parameters, and the good results on the temperature range of interest to this work, we opted for the first approach.

Once the FVT parameters for all the components were determined, one can predict the ηpT data measured in this work. The results of such predictions are shown in Fig. 7. For the system with

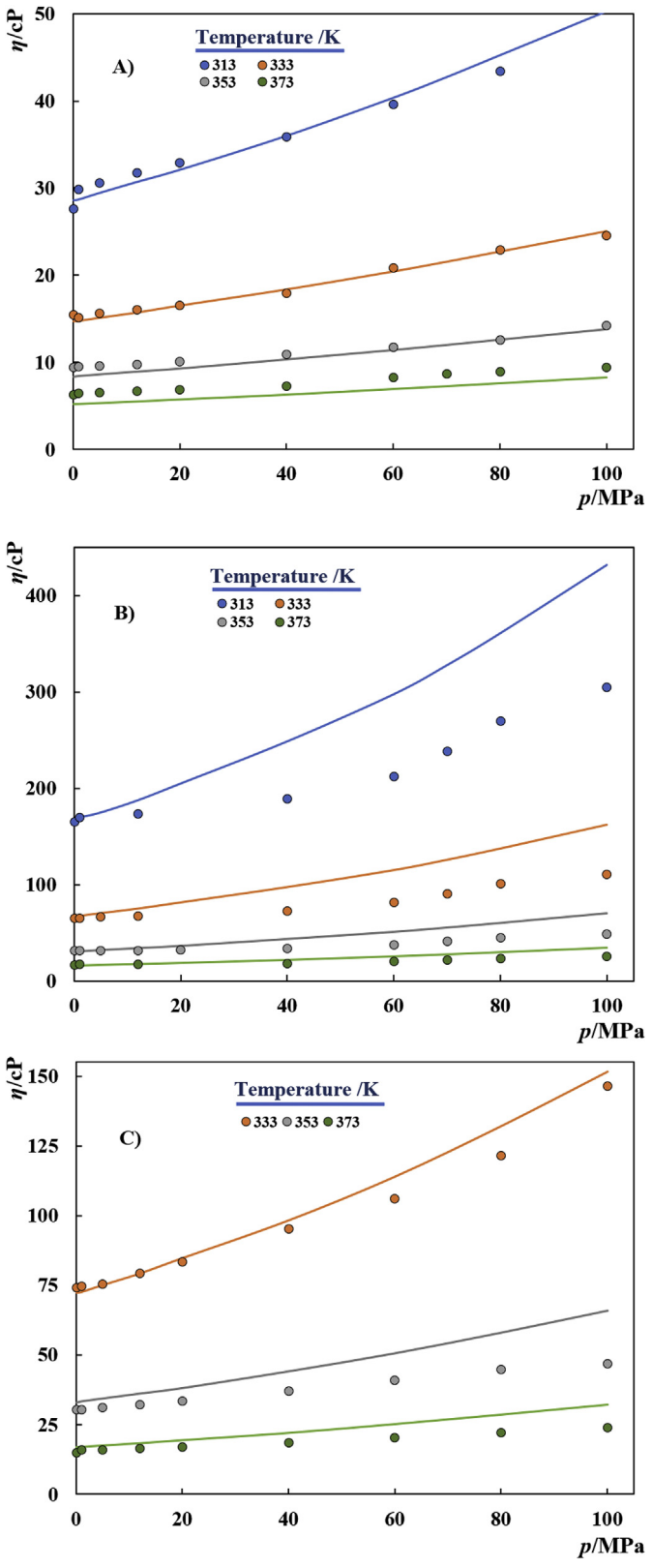

Fig. 7. Viscosities of [Ch]Cl-based DES with different HBDs. A) EG; B) Glycerol; C) Urea. Symbols represent experimental data measured in this work while the solid lines depict the results obtained with PC-SAFT + FVT.

Table 5
Free volume Theory parameters used in this work.

Component	α/J·m^3·mol^{-1} kg^{-1}	B	L_v/Å
Ethylene glycol	379.34	0.002434	0.03301
Glycerol	267.90	0.007701	0.00252
[Ch]Cl	190.54	0.006520	0.08776
Urea	235.94	0.009257	0.00183

$$MAD = \frac{1}{N}\sum_{i=1}^{N}\left|\eta^{calc} - \eta^{\exp}\right| \quad (18)$$

EG, an excellent agreement with the experimental data is observed, showing that both the effect of temperature and pressure is remarkably captured by the PC-SAFT + FVT models proposed here. On the other hand, a considerable overprediction of the pressure effect, more pronounced at lower temperatures, is observed in the system with glycerol. This is expected given the poor description of [Ch]Cl + glycerol (1:2) $p\rho T$ data by PC-SAFT previously discussed and highlight that a good description of the mixture's density has a tremendous effect on the ability of FVT to correlate viscosity data at high pressures. For the system with urea, a reasonable agreement with the experimental data is found although the effect of pressure is poorly described if compared with the system with EG.

Nonetheless, if considering all the experimental viscosity data measured in this work, using the falling body viscometer for the three [Ch]Cl-based DES, overall MADs against the experimental data of 0.81, 22.26, and 4.80 cP were observed for the mixtures with EG, glycerol, and urea, respectively. These deviations increase in the same order as those reported in Table 4 for the PC-SAFT description of the $p\rho T$ data, reinforcing the importance of having an accurate description of $p\rho T$ data in wide temperature and pressure ranges with the chosen EoS prior to the correlation of viscosity data with FVT, which ultimately relies on the development of robust and accurate coarse-grained models for the DES constituents.

For most HBDs used in DES formulations the development of their coarse-grained models is a trivial task as densities and vapor pressures of the pure fluids are available and the model parameterization can be carried following the standard approach in SAFT-type EoS. However, this is not the case for most HBAs and a few HBDs (e.g. urea) which are solid at the range of working temperatures. For this type of compounds, experimental data for the pure fluids are rarely available and alternative approaches are required.

As discussed in the introduction, most literature works dealing with the thermodynamic modelling of DES, using SAFT-type EoS, follow a pseudo-pure component approach where SAFT parameters are regressed to each HBD/HBA combination. Although a pseudo-pure-component approach is an attractive approach to the modelling of some industrially important systems like polymer blends, where the different components are very similar (e.g. different chain length), we consider this approach to be inappropriate for the modelling of DES as they are mixtures of two completely different species. Moreover, it introduces an undesirable compositional dependency on the molecular parameters obtained for the hypothetical pure-component, and in the binary interaction parameters that might be required to describe multi-component systems containing DES. Moreover, solid-liquid equilibrium which is of utmost importance in the framework of DES can't be described under this approach.

Another alternative has been the use of aqueous solutions data (e.g. densities, osmotic coefficients) to regress the parameters for the target compound. Usually aqueous systems are challenging to any thermodynamic model and binary interaction parameters,

sometimes temperature dependent as in the case of [Ch]Cl [56], have to be fitted simultaneously to achieve a good agreement with the experimental data. The inclusion of such parameters may considerably affect the values of the pure-component parameters obtained, which will no longer be able to correctly capture the physical features of the target compound. Hence, and as the results obtained in this work show, the parameters obtained using such diluted data yield inaccurate results when they are applied to describe the density of DES and consequently hinder a good correlation of viscosities. Similar issues are expected if the same models are to be applied to the description of other thermophysical properties or phase equilibria, urging the development of robust and accurate coarse-grained models that are applicable for solid DES precursors. A possible alternative being the use of the more realistic individual-component approach, and the use of high-pressure liquid densities and solid-liquid equilibrium data measured for a representative DES containing the target compound, and a compound that is liquid at room temperature, to obtain the molecular parameters.

5. Conclusions

In this work, densities and viscosities of three archetypical DES, namely [Ch]Cl combined with either EG, glycerol, or urea were measured in wide temperature and pressure ranges, broadening the literature body on the thermophysical characterization of these solvents, especially in what concerns viscosity measurements at high pressure that were here reported for the first time.

Overall, the experimental data measured in this work is in fair agreement with existent data from literature and exhibit the expected trends. Extrapolating the density data measured in this work, the excess molar volumes of the three DES were estimated. The negligible excess molar volume observed in the mixture with urea agrees with the quasi-ideal behavior of [Ch]Cl in urea previously reported in literature, and the highly negative value observed for the system with glycerol agrees with the considerable negative deviations from the ideal behavior reported when studying the solid-liquid equilibrium of this system. Surprisingly, a positive excess molar volume was obtained for the system with EG, suggesting the existence of unfavorable interactions in the system whose existence should be properly investigated in the future.

Moreover, PC-SAFT EoS was coupled to the FVT to correlate the experimental data measured in this work using coarse-grained models of the pure-components readily available in literature that were developed in the framework of research subjects other than DES. The results obtained in this work suggest that the inclusion of appropriate density data in the development of the coarse-grained models of the DES constituents is crucial for a good performance of the model when used to describe DES thermophysical properties.

Hence, considering that many DESs constituents are solid at room temperature and pure fluid densities are not available, other properties are being used in the development of their coarse-grained models. The results obtained here suggest that the diluted aqueous solution data commonly used on such alternative parameterizations yield inaccurate results when used to describe DES, seeming unable to capture the necessary physical information about the size and shape of the molecules. Therefore, alternative approaches to the development of coarse-grained models applicable to the accurate thermodynamic modelling of DES are necessary and should be the focus of future developments on this field.

Acknowledgments

This work was developed within the scope of the project CICECO- Aveiro Institute of Materials, FCT Ref. UID/CTM/50011/2019, financed by national funds through the FCT/MCTES. E. A. Crespo acknowledges FCT for the Ph.D. Grant SFRH/BD/130870/2017. P. J. Carvalho also acknowledges FCT for a contract under the Investigador FCT 2015, contract number IF/00758/2015. B. Soares thanks FCT and The Navigator Co. for the Ph.D. grant SFRH/BDE/103257/2014. The authors gratefully acknowledge Infochem-KBC as the Multiflash software was used in this work for the PC-SAFT EoS calculations.

Appendix A. Supplementary data

Supplementary data to this article can be found online at https://doi.org/10.1016/j.fluid.2019.112249.

References

[1] A.P. Abbott, G. Capper, D.L. Davies, R.K. Rasheed, V. Tambyrajah, Novel solvent properties of choline chloride/urea mixtures, Chem. Commun. (2003) 70–71, https://doi.org/10.1039/b210714g.
[2] M.A.R. Martins, S.P. Pinho, J.A.P. Coutinho, Insights into the nature of eutectic and deep eutectic mixtures, J. Solut. Chem. (2018), https://doi.org/10.1007/s10953-018-0793-1.
[3] E.L. Smith, A.P. Abbott, K.S. Ryder, Deep eutectic solvents (DESs) and their applications, Chem. Rev. 114 (2014) 11060–11082, https://doi.org/10.1021/cr300162p.
[4] M.C. Kroon, D.T. Allen, J.F. Brennecke, P.E. Savage, G.C. Schatz, ACS virtual issue on deep eutectic solvents, J. Chem. Eng. Data 62 (2017) 1927–1928, https://doi.org/10.1021/acs.jced.7b00545.
[5] S.B. Phadtare, G.S. Shankarling, Halogenation reactions in biodegradable solvent: efficient bromination of substituted 1-aminoanthra-9,10-quinone in deep eutectic solvent (choline chloride : urea), Green Chem. 12 (2010) 458–462, https://doi.org/10.1039/B923589B.
[6] P.M. Pawar, K.J. Jarag, G.S. Shankarling, Environmentally benign and energy efficient methodology for condensation: an interesting facet to the classical Perkin reaction, Green Chem. 13 (2011) 2130–2134, https://doi.org/10.1039/C0GC00712A.
[7] N. Azizi, E. Batebi, S. Bagherpour, H. Ghafuri, Natural deep eutectic salt promoted regioselective reduction of epoxides and carbonyl compounds, RSC Adv. 2 (2012) 2289–2293, https://doi.org/10.1039/C2RA01280D.
[8] J.T. Gorke, F. Srienc, R.J. Kazlauskas, Hydrolase-catalyzed biotransformations in deep eutectic solvents, Chem. Commun. (2008) 1235–1237, https://doi.org/10.1039/B716317G.
[9] H. Zhao, G.A. Baker, S. Holmes, New eutectic ionic liquids for lipase activation and enzymatic preparation of biodiesel, Org. Biomol. Chem. 9 (2011) 1908–1916, https://doi.org/10.1039/c0ob01011a.
[10] A.P. Abbott, G. Capper, D.L. Davies, R.K. Rasheed, P. Shikotra, Selective extraction of metals from mixed oxide matrixes using choline-based ionic liquids, Inorg. Chem. 44 (2005) 6497–6499, https://doi.org/10.1021/ic0505450.
[11] N. Schaeffer, M.A.R. Martins, C.M.S.S. Neves, S.P. Pinho, J.A.P. Coutinho, Sustainable hydrophobic terpene-based eutectic solvents for the extraction and separation of metals, Chem. Commun. 54 (2018) 8104–8107, https://doi.org/10.1039/C8CC04152K.
[12] G. Garcia, S. Aparicio, R. Ullah, M. Atilhan, Deep eutectic solvents: physicochemical properties and gas separation applications, Energy Fuel. 29 (2015) 2616–2644, https://doi.org/10.1021/ef5028873.
[13] Y. Zhang, X. Ji, X. Lu, Choline-based deep eutectic solvents for CO2 separation: review and thermodynamic analysis, Renew. Sustain. Energy Rev. 97 (2018) 436–455. https://doi.org/10.1016/j.rser.2018.08.007.
[14] A. Biswas, R.L. Shogren, D.G. Stevenson, J.L. Willett, P.K. Bhowmik, Ionic liquids as solvents for biopolymers: acylation of starch and zein protein, Carbohydr. Polym. 66 (2006) 546–550, https://doi.org/10.1016/j.carbpol.2006.04.005.
[15] H. Zhao, G.A. Baker, Ionic liquids and deep eutectic solvents for biodiesel synthesis: a review, J. Chem. Technol. Biotechnol. 88 (2013) 3–12, https://doi.org/10.1002/jctb.3935.
[16] F.S. Oliveira, A.B. Pereiro, L.P.N. Rebelo, I.M. Marrucho, Deep eutectic solvents as extraction media for azeotropic mixtures, Green Chem. 15 (2013) 1326–1330, https://doi.org/10.1039/C3GC37030E.
[17] F. Pena-Pereira, J. Namieśnik, Ionic liquids and deep eutectic mixtures: sustainable solvents for extraction processes, ChemSusChem 7 (2014) 1784–1800, https://doi.org/10.1002/cssc.201301192.
[18] H.G. Morrison, C.C. Sun, S. Neervannan, Characterization of thermal behavior of deep eutectic solvents and their potential as drug solubilization vehicles, Int. J. Pharm. 378 (2009) 136–139, https://doi.org/10.1016/j.ijpharm.2009.05.039.
[19] H.-G. Liao, Y.-X. Jiang, Z.-Y. Zhou, S.-P. Chen, S.-G. Sun, Shape-controlled synthesis of gold nanoparticles in deep eutectic solvents for studies of structure-functionality relationships in electrocatalysis, Angew Chem. Int.

Ed. Engl. 47 (2008), https://doi.org/10.1002/anie.200803202, 9100–3.
[20] C. Ruß, B. König, Low melting mixtures in organic synthesis – an alternative to ionic liquids? Green Chem. 14 (2012) 2969, https://doi.org/10.1039/c2gc36005e.
[21] B. Tang, K.H. Row, Recent developments in deep eutectic solvents in chemical sciences, Monatshefte Fur Chem. 144 (2013) 1427–1454, https://doi.org/10.1007/s00706-013-1050-3.
[22] Q. Zhang, K. De Oliveira Vigier, S. Royer, F. Jérôme, Deep eutectic solvents: syntheses, properties and applications, Chem. Soc. Rev. 41 (2012) 7108–7146, https://doi.org/10.1039/c2cs35178a.
[23] I. Adeyemi, M.R.M. Abu-Zahra, I. Alnashef, Experimental study of the solubility of CO2 in novel amine based deep eutectic solvents, Energy Procedia 105 (2017) 1394–1400. https://doi.org/10.1016/j.egypro.2017.03.519.
[24] H. Srinivasan, P.S. Dubey, V.K. Sharma, R. Biswas, S. Mitra, R. Mukhopadhyay, Molecular dynamics of acetamide based ionic deep eutectic solvents, AIP Conf. Proc. 1942 (2018) 110032, https://doi.org/10.1063/1.5029015.
[25] A.P. Abbott, D. Boothby, G. Capper, D.L. Davies, R.K. Rasheed, Deep Eutectic Solvents formed between choline chloride and carboxylic acids: versatile alternatives to ionic liquids, J. Am. Chem. Soc. 126 (2004) 9142–9147, https://doi.org/10.1021/ja048266j.
[26] C. Florindo, F.S. Oliveira, L.P.N. Rebelo, A.M. Fernandes, I.M. Marrucho, Insights into the synthesis and properties of deep eutectic solvents based on choline chloride and carboxylic acids, ACS Sustain. Chem. Eng. 2 (2014) 2416–2425, https://doi.org/10.1021/sc500439w.
[27] D.J.G.P. van Osch, L.F. Zubeir, A. van den Bruinhorst, M.A.A. Rocha, M.C. Kroon, Hydrophobic deep eutectic solvents as water-immiscible extractants, Green Chem. 17 (2015) 4518–4521, https://doi.org/10.1039/C5GC01451D.
[28] P.V.A. Pontes, E.A. Crespo, M.A.R. Martins, L.P. Silva, C.M.S.S. Neves, G.J. Maximo, M.D. Hubinger, E.A.C. Batista, S.P. Pinho, J.A.P. Coutinho, G. Sadowski, C. Held, Measurement and PC-SAFT modeling of solid-liquid equilibrium of deep eutectic solvents of quaternary ammonium chlorides and carboxylic acids, Fluid Phase Equilib. 448 (2017) 69–80, https://doi.org/10.1016/j.fluid.2017.04.007.
[29] E.A. Crespo, L.P. Silva, M.A.R. Martins, M. Bülow, O. Ferreira, G. Sadowski, C. Held, S.P. Pinho, J.A.P. Coutinho, The role of polyfunctionality in the formation of [Ch]Cl-carboxylic acid-based deep eutectic solvents, Ind. Eng. Chem. Res. 57 (2018) 11195–11209, https://doi.org/10.1021/acs.iecr.8b01249.
[30] K. Shahbaz, F.S. Mjalli, M.A. Hashim, I.M. Al-Nashef, Using deep eutectic solvents for the removal of glycerol from palm oil-based biodiesel, J. Appl. Sci. 10 (2010) 3349–3354.
[31] K. Shahbaz, F.S. Mjalli, Ma Hashim, I.M. AlNashef, Prediction of deep eutectic solvents densities at different temperatures, Thermochim. Acta 515 (2011) 67–72.
[32] Y.H. Choi, J. Van Spronsen, Y. Dai, M. Verbene, F. Hollmann, I.W.C.E. Arends, G.J. Witkamp, R. Verpoorte, Are natural deep eutectic solvents the missing link in understanding cellular metabolism and physiology? Plant Physiol. 156 (2011) 1701–1705, https://doi.org/10.1104/pp.111.178426.
[33] J. Parnica, M. Antalik, Urea and guanidine salts as novel components for deep eutectic solvents, J. Mol. Liq. 197 (2014) 23–26, https://doi.org/10.1016/J.MOLLIQ.2014.04.016.
[34] Z. Maugeri, P. Dominguez de Maria, Novel choline-chloride-based deep-eutectic-solvents with renewable hydrogen bond donors: levulinic acid and sugar-based polyols, RSC Adv. 2 (2012) 421–425, https://doi.org/10.1039/C1RA00630D.
[35] L.P. Silva, L. Fernandez, J.H.F. Conceição, M.A.R. Martins, A. Sosa, J. Ortega, S.P. Pinho, J.A.P. Coutinho, Design and characterization of sugar-based deep eutectic solvents using conductor-like screening model for real solvents, ACS Sustain. Chem. Eng. 6 (2018) 10724–10734, https://doi.org/10.1021/acssuschemeng.8b02042.
[36] O. Ciocirlan, O. Iulian, O. Croitoru, Effect of temperature on the physico-chemical properties of three ionic liquids containing choline chloride, Rev. Chim. (Bucharest) 61 (2010) 721–723.
[37] R.B. Leron, A.N. Soriano, M.H. Li, Densities and refractive indices of the deep eutectic solvents (choline chloride+ethylene glycol or glycerol) and their aqueous mixtures at the temperature ranging from 298.15 to 333.15K, J. Taiwan Inst. Chem. Eng. 43 (2012) 551–557, https://doi.org/10.1016/j.jtice.2012.01.007.
[38] K. Shahbaz, S. Baroutian, F.S. Mjalli, M.A. Hashim, I.M. Alnashef, Densities of ammonium and phosphonium based deep eutectic solvents: prediction using artificial intelligence and group contribution techniques, Thermochim. Acta 527 (2012) 59–66, https://doi.org/10.1016/j.tca.2011.10.010.
[39] A. Popescu, Density, viscosity and electrical conductivity of three choline chloride based ionic liquids, Bulg. Chem. 46 (2014) 452–457.
[40] F.S. Mjalli, G. Vakili-Nezhaad, K. Shahbaz, I.M. AlNashef, Application of the Eötvos and Guggenheim empirical rules for predicting the density and surface tension of ionic liquids analogues, Thermochim. Acta 575 (2014) 40–44. https://doi.org/10.1016/j.tca.2013.10.017.
[41] A. Yadav, J.R. Kar, M. Verma, S. Naqvi, S. Pandey, Densities of aqueous mixtures of (choline chloride+ethylene glycol) and (choline chloride+malonic acid) deep eutectic solvents in temperature range 283.15–363.15K, Thermochim. Acta 600 (2015) 95–101, https://doi.org/10.1016/j.tca.2014.11.028.
[42] F.S. Mjalli, O.U. Ahmed, Ethaline and Glyceline binary eutectic mixtures: characteristics and intermolecular interactions, Asia-Pacific, J. Chem. Eng. 12 (2017) 313–320, https://doi.org/10.1002/apj.2074.
[43] A.R. Harifi-Mood, R. Buchner, Density, viscosity, and conductivity of choline chloride+ethylene glycol as a deep eutectic solvent and its binary mixtures with dimethyl sulfoxide, J. Mol. Liq. 225 (2017) 689–695. https://doi.org/10.1016/j.molliq.2016.10.115.
[44] A. Yadav, S. Trivedi, R. Rai, S. Pandey, Densities and dynamic viscosities of (choline chloride+glycerol) deep eutectic solvent and its aqueous mixtures in the temperature range (283.15–363.15)K, Fluid Phase Equilib. 367 (2014) 135–142. https://doi.org/10.1016/j.fluid.2014.01.028.
[45] M.K. Alomar, M. Hayyan, M.A. Alsaadi, S. Akib, A. Hayyan, M.A. Hashim, Glycerol-based deep eutectic solvents: physical properties, J. Mol. Liq. 215 (2016) 98–103, https://doi.org/10.1016/j.molliq.2015.11.032.
[46] A.-M. Popescu, V. Constantin, A. Florea, A. Baran, Physical and electrochemical properties of 2-hydroxy-ethyl-trimethyl ammonium chloride based ionic liquids as potential electrolytes for metals electrodeposition, Rev. Chim. (Bucharest) 62 (2011) 531–537.
[47] A. Yadav, S. Pandey, Densities and viscosities of (choline chloride + urea) deep eutectic solvent and its aqueous mixtures in the temperature range 293.15 K to 363.15 K, J. Chem. Eng. Data 59 (2014) 2221–2229, https://doi.org/10.1021/je5001796.
[48] R.B. Leron, M.-H. Li, High-pressure volumetric properties of choline chloride–ethylene glycol based deep eutectic solvent and its mixtures with water, Thermochim. Acta 546 (2012) 54–60. https://doi.org/10.1016/j.tca.2012.07.024.
[49] R.B. Leron, D.S.H. Wong, M.-H. Li, Densities of a deep eutectic solvent based on choline chloride and glycerol and its aqueous mixtures at elevated pressures, Fluid Phase Equilib. 335 (2012) 32–38. https://doi.org/10.1016/j.fluid.2012.08.016.
[50] R.B. Leron, M.-H. Li, High-pressure density measurements for choline chloride: urea deep eutectic solvent and its aqueous mixtures at T=(298.15 to 323.15)K and up to 50MPa, J. Chem. Thermodyn. 54 (2012) 293–301. https://doi.org/10.1016/j.jct.2012.05.008.
[51] C. D'Agostino, R.C. Harris, A.P. Abbott, L.F. Gladden, M.D. Mantle, Molecular motion and ion diffusion in choline chloride based deep eutectic solvents studied by 1H pulsed field gradient NMR spectroscopy, Phys. Chem. Chem. Phys. 13 (2011) 21383–21391, https://doi.org/10.1039/C1CP22554E.
[52] A.P. Abbott, R.C. Harris, K.S. Ryder, C. D'Agostino, L.F. Gladden, M.D. Mantle, Glycerol eutectics as sustainable solvent systems, Green Chem. 13 (2011) 82–90, https://doi.org/10.1039/C0GC00395F.
[53] W.G. Chapman, K.E. Gubbins, G. Jackson, M. Radosz, SAFT: equation-of-state solution model for associating fluids, Fluid Phase Equilib. 52 (1989) 31–38, https://doi.org/10.1016/0378-3812(89)80308-5.
[54] W.G. Chapman, K.E. Gubbins, G. Jackson, M. Radosz, New reference equation of state for associating liquids, Ind. Eng. Chem. Res. 29 (1990) 1709–1721, https://doi.org/10.1021/ie00104a021.
[55] S.P. Verevkin, A.Y. Sazonova, A.K. Frolkova, D.H. Zaitsau, I.V. Prikhodko, C. Held, Separation performance of BioRenewable deep eutectic solvents, Ind. Eng. Chem. Res. 54 (2015) 3498–3504, https://doi.org/10.1021/acs.iecr.5b00357.
[56] L.F. Zubeir, C. Held, G. Sadowski, M.C. Kroon, PC-SAFT modeling of CO2 solubilities in deep eutectic solvents, J. Phys. Chem. B 120 (2016) 2300–2310, https://doi.org/10.1021/acs.jpcb.5b07888.
[57] C.H.J.T. Dietz, D.J.G.P. van Osch, M.C. Kroon, G. Sadowski, M. van Sint Annaland, F. Gallucci, L.F. Zubeir, C. Held, PC-SAFT modeling of CO2 solubilities in hydrophobic deep eutectic solvents, Fluid Phase Equilib. 448 (2017) 94–98, https://doi.org/10.1016/J.FLUID.2017.03.028.
[58] S.E.E. Warrag, C. Pototzki, N.R. Rodriguez, M. van Sint Annaland, M.C. Kroon, C. Held, G. Sadowski, C.J. Peters, Oil desulfurization using deep eutectic solvents as sustainable and economical extractants via liquid-liquid extraction: experimental and PC-SAFT predictions, Fluid Phase Equilib. 467 (2018) 33–44, https://doi.org/10.1016/J.FLUID.2018.03.018.
[59] R. Haghbakhsh, S. Raeissi, Modeling the phase behavior of carbon dioxide solubility in deep eutectic solvents with the cubic plus association equation of state, J. Chem. Eng. Data 63 (2018) 897–906, https://doi.org/10.1021/acs.jced.7b00472.
[60] E.A. Crespo, L.P. Silva, M.A.R. Martins, L. Fernandez, J. Ortega, O. Ferreira, G. Sadowski, C. Held, S.P. Pinho, J.A.P. Coutinho, Characterization and modeling of the liquid phase of deep eutectic solvents based on fatty acids/alcohols and choline chloride, Ind. Eng. Chem. Res. 56 (2017) 12192–12202, https://doi.org/10.1021/acs.iecr.7b02382.
[61] R.M. Ojeda, F. Llovell, Soft-saft transferable molecular models for the description of gas solubility in eutectic ammonium salt-based solvents, J. Chem. Eng. Data (2018), https://doi.org/10.1021/acs.jced.7b01103.
[62] A. Allal, C. Boned, A. Baylaucq, Free-volume viscosity model for fluids in the dense and gaseous states, Phys. Rev. E. 64 (2001) 11203, https://doi.org/10.1103/PhysRevE.64.011203.
[63] A. Allal, M. Moha-ouchane, C. Boned, A new free volume model for dynamic viscosity and density of dense fluids versus pressure and temperature, Phys. Chem. Liq. 39 (2001) 1–30, https://doi.org/10.1080/00319100108030323.
[64] S.E. Quiñones-Cisneros, C.K. Zéberg-Mikkelsen, E.H. Stenby, The friction theory (f-theory) for viscosity modeling, Fluid Phase Equilib. 169 (2000) 249–276. https://doi.org/10.1016/S0378-3812(00)00310-1.
[65] S.E. Quiñones-Cisneros, C.K. Zéberg-Mikkelsen, E.H. Stenby, One parameter friction theory models for viscosity, Fluid Phase Equilib. 178 (2001) 1–16. https://doi.org/10.1016/S0378-3812(00)00474-X.

[66] R. Haghbakhsh, K. Parvaneh, S. Raeissi, A. Shariati, A general viscosity model for deep eutectic solvents: the free volume theory coupled with association equations of state, Fluid Phase Equilib. 470 (2018) 193–202, https://doi.org/10.1016/J.FLUID.2017.08.024.
[67] R. Haghbakhsh, S. Raeissi, K. Parvaneh, A. Shariati, The friction theory for modeling the viscosities of deep eutectic solvents using the CPA and PC-SAFT equations of state, J. Mol. Liq. 249 (2018) 554–561, https://doi.org/10.1016/J.MOLLIQ.2017.11.054.
[68] J.O. Lloret, L.F. Vega, F. Llovell, Accurate description of thermophysical properties of Tetraalkylammonium Chloride Deep Eutectic Solvents with the soft-SAFT equation of state, Fluid Phase Equilib. 448 (2017) 81–93. https://doi.org/10.1016/j.fluid.2017.04.013.
[69] E.A. Crespo, J.M.L. Costa, Z.B.M.A. Hanafiah, K.A. Kurnia, M.B. Oliveira, F. Llovell, L.F. Vega, P.J. Carvalho, J.A.P. Coutinho, New measurements and modeling of high pressure thermodynamic properties of glycols, Fluid Phase Equilib. 436 (2017) 113–123, https://doi.org/10.1016/j.fluid.2017.01.003.
[70] P.J. Carvalho, T. Regueira, L.M.N.B.F. Santos, J. Fernandez, J.A.P. Coutinho, Effect of water on the viscosities and densities of 1-Butyl-3-methylimidazolium dicyanamide and 1-Butyl-3-methylimidazolium tricyanomethane at atmospheric pressure, J. Chem. Eng. Data 55 (2010) 645–652, https://doi.org/10.1021/je900632q.
[71] F.M. Gaciño, M.J.P. Comuñas, T. Regueira, J.J. Segovia, J. Fernández, On the viscosity of two 1-butyl-1-methylpyrrolidinium ionic liquids: effect of the temperature and pressure, J. Chem. Thermodyn. 87 (2015) 43–51. https://doi.org/10.1016/j.jct.2015.03.002.
[72] E.I. Concepción, Á. Gómez-Hernández, M.C. Martín, J.J. Segovia, Density and viscosity measurements of aqueous amines at high pressures: DEA-water, DMAE-water and TEA-water mixtures, J. Chem. Thermodyn. 112 (2017) 227–239. https://doi.org/10.1016/j.jct.2017.05.001.
[73] J.R. Zambrano, M. Sobrino, M.C. Martín, M.A. Villamañán, C.R. Chamorro, J.J. Segovia, Contributing to accurate high pressure viscosity measurements: vibrating wire viscometer and falling body viscometer techniques, J. Chem. Thermodyn. 96 (2016) 104–116. https://doi.org/10.1016/j.jct.2015.12.021.
[74] J. Gross, G. Sadowski, Perturbed-chain SAFT: an equation of state based on a perturbation theory for chain molecules, Ind. Eng. Chem. Res. 40 (2001) 1244–1260, https://doi.org/10.1021/ie0003887.
[75] G. Jackson, W.G. Chapman, K.E. Gubbins, Phase equilibria of associating fluids of spherical and chain molecules, Int. J. Thermophys. 9 (1988) 769–779, https://doi.org/10.1007/BF00503243.
[76] W.G. Chapman, G. Jackson, K.E. Gubbins, Phase equilibria of associating fluids. Chain molecules with multiple bonding sites, Mol. Phys. 65 (1988) 1057–1079.
[77] M.S. Wertheim, Fluids with highly directional attractive forces. I. Statistical thermodynamics, J. Stat. Phys. 35 (1984) 19–34, https://doi.org/10.1007/BF01017362.
[78] M.S. Wertheim, Fluids with highly directional attractive forces. II. Thermodynamic perturbation theory and integral equations, J. Stat. Phys. 35 (1984) 35–47, https://doi.org/10.1007/BF01017363.
[79] M.S. Wertheim, Fluids with highly directional attractive forces. III. Multiple attraction sites, J. Stat. Phys. 42 (1986) 459–476, https://doi.org/10.1007/BF01127721.
[80] M.S. Wertheim, Fluids with highly directional attractive forces. IV. Equilibrium polymerization, J. Stat. Phys. 42 (1986) 477–492, https://doi.org/10.1007/BF01127722.
[81] J.A. Barker, D. Henderson, Perturbation theory and equation of state for fluids: the square-well potential, J. Chem. Phys. 47 (1967) 2856–2861.
[82] J.A. Barker, D. Henderson, Perturbation theory and equation of state for fluids. II. A successful theory of liquids, J. Chem. Phys. 47 (1967) 4714–4721.
[83] J.P. Wolbach, S.I. Sandler, Using molecular orbital calculations to describe the phase behavior of cross-associating mixtures, Ind. Eng. Chem. Res. 37 (1998) 2917–2928, https://doi.org/10.1021/ie970781l.
[84] C. Held, T. Neuhaus, G. Sadowski, Compatible solutes: thermodynamic properties and biological impact of ectoines and prolines, Biophys. Chem. 152 (2010) 28–39, https://doi.org/10.1016/j.bpc.2010.07.003.
[85] C. Held, G. Sadowski, Compatible solutes: thermodynamic properties relevant for effective protection against osmotic stress, Fluid Phase Equilib. 407 (2016) 224–235. https://doi.org/10.1016/j.fluid.2015.07.004.
[86] M. Atilhan, S. Aparicio, PρT measurements and derived properties of liquid 1,2-alkanediols, J. Chem. Thermodyn. 57 (2013) 137–144. https://doi.org/10.1016/j.jct.2012.08.014.
[87] T. Reschke, C. Brandenbusch, G. Sadowski, Modeling aqueous two-phase systems: I. Polyethylene glycol and inorganic salts as ATPS former, Fluid Phase Equilib. 368 (2014) 91–103, https://doi.org/10.1016/j.fluid.2014.02.016.
[88] X. Liang, W. Yan, K. Thomsen, G.M. Kontogeorgis, Modeling the liquid–liquid equilibrium of petroleum fluid and polar compounds containing systems with the PC-SAFT equation of state, Fluid Phase Equilib. 406 (2015) 147–155. https://doi.org/10.1016/j.fluid.2015.07.042.
[89] T.H. Chung, M. Ajlan, L.L. Lee, K.E. Starling, Generalized multiparameter correlation for nonpolar and polar fluid transport properties, Ind. Eng. Chem. Res. 27 (1988) 671–679, https://doi.org/10.1021/ie00076a024.
[90] P.D. Neufeld, A.R. Janzen, R.A. Aziz, Empirical equations to calculate 16 of the transport collision integrals Ω(l,s)* for the Lennard-Jones (12–6) potential, J. Chem. Phys. 57 (1972) 1100–1102, https://doi.org/10.1063/1.1678363.
[91] C.R. Wilke, A viscosity equation for gas mixtures, J. Chem. Phys. 18 (1950) 517–519, https://doi.org/10.1063/1.1747673.
[92] L.M.C. Pereira, F. Llovell, L.F. Vega, Thermodynamic characterisation of aqueous alkanolamine and amine solutions for acid gas processing by transferable molecular models, Appl. Energy 222 (2018) 687–703, https://doi.org/10.1016/J.APENERGY.2018.04.021.
[93] X. Canet, P. Daugé, A. Baylaucq, C. Boned, C.K. Zéberg-Mikkelsen, S.E. Quiñones-Cisneros, E.H. Stenby, Density and viscosity of the 1-methylnaphthalene+2,2,4,4,6,8,8-Heptamethylnonane system from 293.15 to 353.15 K at pressures up to 100 MPa, Int. J. Thermophys. 22 (2001) 1669–1689, https://doi.org/10.1023/A:1013182715406.
[94] C. Boned, C.K. Zéberg-Mikkelsen, A. Baylaucq, P. Daugé, High-pressure dynamic viscosity and density of two synthetic hydrocarbon mixtures representative of some heavy petroleum distillation cuts, Fluid Phase Equilib. 212 (2003) 143–164. https://doi.org/10.1016/S0378-3812(03)00279-6.
[95] A. Baylaucq, C. Boned, X. Canet, C.K. Zéberg-Mikkelsen, High-pressure (up to 140 MPa) dynamic viscosity of the methane and toluene system: measurements and comparative study of some representative models, Int. J. Thermophys. 24 (2003) 621–638, https://doi.org/10.1023/A:1024023913165.
[96] M.A. Monsalvo, A. Baylaucq, P. Reghem, S.E. Quiñones-Cisneros, C. Boned, Viscosity measurements and correlations of binary mixtures: 1,1,1,2-tetrafluoroethane (HFC-134a)+tetraethylene glycol dimethylether (TEGDME), Fluid Phase Equilib. 233 (2005) 1–8. https://doi.org/10.1016/j.fluid.2005.03.030.
[97] A. Baylaucq, C. Boned, X. Canet, C.K. Zéberg-Mikkelsen, S.E. Quiñones-Cisneros, H. Zhou, Dynamic viscosity modeling of methane + n-decane and methane + toluene Mixtures : comparative study of some representative models, Pet. Sci. Technol. 23 (2005) 143–157, https://doi.org/10.1081/LFT-200028122.
[98] C.K. Zéberg-Mikkelsen, G. Watson, A. Baylaucq, G. Galliéro, C. Boned, Comparative experimental and modeling studies of the viscosity behavior of ethanol+C7 hydrocarbon mixtures versus pressure and temperature, Fluid Phase Equilib. 245 (2006) 6–19. https://doi.org/10.1016/j.fluid.2006.01.030.
[99] N. Cain, G. Roberts, D. Kiserow, R. Carbonell, Modeling the thermodynamic and transport properties of decahydronaphthalene/propane mixtures: phase equilibria, density, and viscosity, Fluid Phase Equilib. 305 (2011) 25–33. https://doi.org/10.1016/j.fluid.2011.02.009.
[100] T.E. Daubert, H.M. Sibul, C.C. Stebbins, R.P. Danner, R.L. Rowley, M.E. Adams, W. V Wilding, T.L. Marshall, Physical and Thermodynamic Properties of Pure Chemicals: DIPPR: Data Compilation: Core + Supplements 1-10, Taylor & Francis, 2000. https://books.google.pt/books?id=MQOjPQAACAAJ.
[101] M. Francisco, A.S.B. Gonzalez, S.L. Garcia de Dios, W. Weggemans, M.C. Kroon, Comparison of a low transition temperature mixture (LTTM) formed by lactic acid and choline chloride with choline lactate ionic liquid and the choline chloride salt: physical properties and vapour-liquid equilibria of mixtures containing water and ethanol, RSC Adv. 3 (2013) 23553–23561, https://doi.org/10.1039/C3RA40303C.
[102] C.F. Araujo, J.A.P. Coutinho, M.M. Nolasco, S.F. Parker, P.J.A. Ribeiro-Claro, S. Rudic, B.I.G. Soares, P.D. Vaz, Inelastic neutron scattering study of reline: shedding light on the hydrogen bonding network of deep eutectic solvents, Phys. Chem. Chem. Phys. 19 (2017) 17998–18009, https://doi.org/10.1039/C7CP01286A.
[103] A.P. Abbott, P.M. Cullis, M.J. Gibson, R.C. Harris, E. Raven, Extraction of glycerol from biodiesel into a eutectic based ionic liquid, Green Chem. 9 (2007) 868–872, https://doi.org/10.1039/B702833D.
[104] X. Meng, K. Ballerat-Busserolles, P. Husson, J.-M. Andanson, Impact of water on the melting temperature of urea + choline chloride deep eutectic solvent, New J. Chem. 40 (2016) 4492–4499, https://doi.org/10.1039/C5NJ02677F.
[105] D.I. Sagdeev, M.G. Fomina, G.K. Mukhamedzyanov, I.M. Abdulagatov, Experimental study of the density and viscosity of polyethylene glycols and their mixtures at temperatures from 293K to 465K and at high pressures up to 245MPa, Fluid Phase Equilib. 315 (2012) 64–76. https://doi.org/10.1016/j.fluid.2011.11.022.